HIGHLY SENSITIVE DETECTION OF LEAD IN AQUEOUS SOLUTION USING LASER-INDUCED BREAKDOWN SPECTROSCOPY COUPLED WITH ADSORPTION TECHNIQUE **

A. F. M. Y. Haider [1,2], M. Parvin [1], Z. H. Khan [1*], M. Wahadoszamen [1]

[1] Department of Physics, University of Dhaka, Dhaka, Bangladesh
[2] Department of Mathematics and Natural Sciences, BRAC University, Dhaka, Bangladesh;
e-mail: zulfiqarshuvo@du.ac.bd

Two types of adsorbents, zinc oxide (ZnO) and zeolite, have been used to probe the lowest detectable limit of lead (Pb) dissolved in water. To achieve the goal, water-soluble Pb complexes were produced by dissolving in water or titrating with HNO_3 acid with different concentrations of four different compounds of Pb. The dissolved Pb complexes were then allowed to be adsorbed onto ZnO or zeolite. LIBS spectra of the Pb-ZnO and Pb-zeolite composites were recorded in the 331.5–370.5, and 355–394 nm spectral windows, respectively. Calibration curves were drawn using the normalized line intensities of Pb I at wavelengths of 357.269, 363.958, and 368.319 nm versus the concentration of the added Pb. For all the adsorbates (the Pb compounds) used, the adsorption curves as a function of the adsorbate concentration in water followed the Langmuir type isotherms. The lowest limit of detection (LoD) and the slope of the linear part of the adsorption isotherm varied for various adsorbents, adsorbates, and different Pb I emission lines used. ZnO was found to be a better adsorbent than zeolite in terms of LoD and the slope of the linear part of the isotherm and hence the sensitivity of the detection. The LoD for Pb in an aqueous solution in the current LIBS experiment coupled with the adsorption technique was found to be 0.5 ppm.

Keywords: *laser-induced breakdown spectroscopy, adsorbent, ZnO, zeolite, lead.*

ВЫСОКОЧУВСТВИТЕЛЬНОЕ ОБНАРУЖЕНИЕ СВИНЦА В ВОДНОМ РАСТВОРЕ МЕТОДОМ ЛАЗЕРНО-ИСКРОВОЙ СПЕКТРОСКОПИИ С ПРИМЕНЕНИЕМ АДСОРБЦИИ

A. F. M. Y. Haider [1,2], M. Parvin [1], Z. H. Khan [1*], M. Wahadoszamen [1]

УДК 543.42:546.815/.819

[1] Даккский Университет, Дакка, Бангладеш
[2] Университет BRAC, Дакка, Бангладеш; e-mail: zulfiqarshuvo@du.ac.bd

(Поступила 30 сентября 2019)

Для установления нижнего предела обнаружения свинца, растворенного в воде, использованы два типа адсорбентов — оксид цинка (ZnO) и цеолит. Водорастворимые комплексы Pb получены путем растворения четырех различных соединений Pb в воде либо титрования кислотой HNO_3 с различной концентрацией. Растворенные комплексы Pb адсорбировали на ZnO или цеолите. Спектры LIBS композитов Pb-ZnO и Pb-цеолит зарегистрированы в диапазонах 331.5–370.5 и 355–394 нм. Калибровочные кривые построены с использованием нормированных интенсивностей линий Pb I на λ = 357.269, 363.958 и 368.319 нм в зависимости от концентрации добавленного Pb. Для всех используемых адсорбатов (соединений Pb) кривые адсорбции в зависимости от концентрации адсорбата в воде соответствуют изотермам ленгмюровского типа. Нижний предел обнаружения (LoD) и наклон линейной части изотермы адсорбции варьируют для различных адсорбентов, адсорбатов и используемых линий эмиссии PbI. Обнаружено, что ZnO лучший адсорбент, чем цеолит, с точки зрения LoD и наклона линейной части изотермы и, следовательно, чувствительности обнаружения. Нижний предел обнаружения Pb в водном растворе при применении лазерно-искровой спектроскопии в сочетании с методом адсорбции 0.5 частиц/млн.

Ключевые слова: *лазерно-искровая спектроскопия, адсорбент, ZnO, цеолит, свинец.*

** Full text is published in JAS V. 87, No. 6 (http://springer.com/journal/10812) and in electronic version of ZhPS V. 87, No. 6 (http://www.elibrary.ru/title_about.asp?id=7318; sales@elibrary.ru).

Introduction. Laser-induced breakdown spectroscopy (LIBS) is a well-established atomic emission spectroscopic technique that uses a high-power pulsed laser to generate a weakly ionized plasma of the sample under investigation. As this plasma expands and cools, characteristic atomic/ionic spectral lines are emitted by the excited atomic/ionic species in the micro-plasma generated from the sample. Since the LIBS emission lines of a specimen solely originate from its excited atomic/ionic species, the elemental composition of the specimen can easily be determined by analyzing its LIBS spectra. LIBS has a unique ability to perform a multi-elemental real-time analysis, which is not possible by any other conventional method. Inter alia, owing to its exceptional capability to perform simultaneous qualitative and quantitative elemental analyses [1–4], LIBS has become nowadays a convenient experimental technique for numerous applications such as mineral analysis [5, 6], detection of biologically hazardous elements [7, 8], analysis of biological samples [9, 10], biomedical analysis [11], space exploration [12], and on-line analysis of industrial products [13].

Although the LIBS technique has compelling advantages in elemental analysis and profiling, the detection of trace elements in ppm or sub-ppm levels in water by in situ LIBS is still a challenging task. This difficulty stems mostly from the fact that when the laser pulse is focused on the surface or inside the liquid, water splashes and severely interferes with both detection and focusing optics. Besides, the emission lines from the plasma are often confined to a limited region or extinct by the surrounding liquid layer, leading to rapid quenching of the characteristic atomic emission line intensities [14–17].

To circumvent these limitations and to enhance the signal-to-noise (S/N) ratio as well as to improve the LoD, several techniques have been reported in the literature, such as the liquid jet LIBS technique [13, 18, 19], the double-pulse LIBS system, and a combination of LIBS with laser induced fluorescence [20]. However, these techniques usually employ complex and expensive analytical equipment with insufficient detection sensitivity. This problem can be significantly alleviated if we adsorb the dissolved trace element by a suitable adsorbent and take a LIBS spectrum of the solid matrix of the adsorbent and the adsorbates [8].

The concentration of the trace element in the solid matrix of the adsorbent can be increased significantly using a suitable adsorbent, and this liquid-to-solid conversion of the samples is advantageous for easier and inexpensive detection. For example, Zhu et al. [21] detected trace Pb in a liquid solution by LIBS using bamboo charcoal as an adsorbent. Knopp et al. [22] found that the detection limit of Pb^{2+} in $Pb(CH_3COO)_2.Pb(OH)_2$ salt solution is 12.5 ppm. Other examples of the liquid-to-solid conversion of the samples used wood slice [23], carbon planchet [15], porous electrospun ultrafine fibre [24], 3D nanochannel porous membrane [24], metallic substrate [25], and calcium hydroxide pellet [26]. Recently, Liu et al. [27] demonstrated that the LoD of Pb could be as low as 3.5 ng/mL using metal-chelate (diethyldithiocarbamate) induced gold nanoparticle aggregation enhanced LIBS. However, some instruments used in the preparation procedure were relatively expensive, and the sample preparation procedures were complicated [17, 20, 28]. In another work, surface-enhanced laser-induced breakdown spectroscopy (SENLIBS) was applied to detect Pb in an aqueous solution on a Zn substrate, and the corresponding LoD was 0.004 mg/L [29].

With the rapid development of industries such as fossil-fuel power stations, battery manufacturing, textile dyeing, and organic chemical manufacturing in Bangladesh, an excessive amount of heavy metals is poured into the ecosystem. The rampant dumping of industrial effluent containing Pb imposes a severe threat to fish, aquatic microorganisms, and other living bodies and contaminates the adjacent soil. The Pb contamination enters the food chain, posing a significant challenge to the overall biodiversity of the surrounding areas. Long-term exposure to Pb is deleterious for health and can increase the risk of irregular high blood pressure and kidney damage. In particular, the development of the brain and nervous systems of children is greatly affected due to long-term exposure to Pb [30, 31]. Therefore, periodic monitoring of the concentration of heavy metals like Pb in the surrounding aquatic environment is of utmost importance. For this purpose, LIBS, coupled with adsorption, could be a sensitive, low-cost, and time-saving practical approach towards detecting water dissolved sub-ppm level of Pb.

In the present work, two types of adsorbent, ZnO and zeolite, have been used to improve the detection limit of Pb in water by LIBS. Since adsorption occurs only at the surface of the adsorbent, the concentration of trace elements on the surface of the adsorbent becomes sufficient to be easily detected by LIBS.

Experimental. A schematic diagram of the experimental setup is shown in Fig. 1. The 2nd harmonic of a Q-switched Nd:YAG (Spectra-Physics LAB-170-10) laser at 532 nm with a pulse duration of 8 ns, repetition rate of 10 Hz, and a variable pulse energy was focused on a circular spot of about 100 μm in radius on the target sample by a convex lens of 10 cm focal length. The focused laser pulses generated an intense, transient, and weakly ionized micro-plasma. The actual pulse energy used was 40 mJ. The beam had a Gaussian profile in the far-field with a beam divergence of less than 0.5 mrad. The experiments were performed in the air [32].

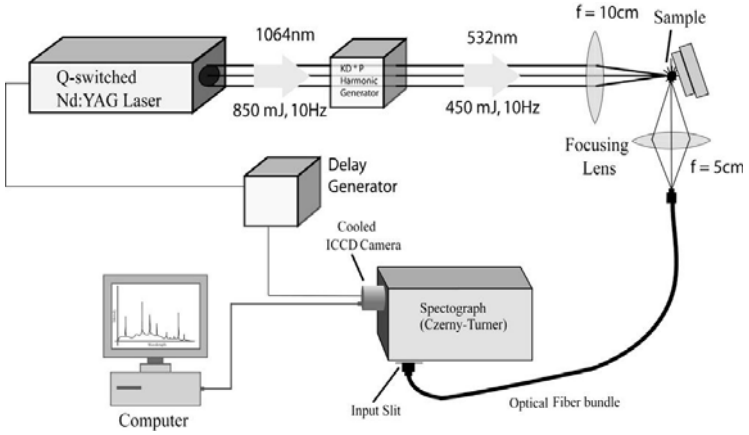

Fig. 1. Schematic diagram of the LIBS experimental setup.

The light emitted from the plasma was focused using a fused quartz lens (f = 5 cm) and collected at the input of a 300 cm long multimode silica fiber. The output of the optical fiber was placed at the entrance slit of a 75 cm focal length computerized Czerny–Turner spectrograph (Acton Model SP-2758). The spectrograph was equipped with three ruled gratings: 2400, 600, and 300 grooves/mm blazed at 240, 500, and 300 nm, respectively, which were interchangeable under computer control, providing high- and low-resolution spectra in the wavelength range 190–880 nm. In the present work, the 600 grooves/mm grating was used, covering a spectral window of 39 nm (331.5–370.5 nm for ZnO and 355–394 nm for zeolite) [8].

A gated and intensified CCD camera (ICCD camera, Princeton PI-MAX with Unigen II coating and programmable delay generator) was coupled to the spectrograph's output. The ICCD camera had 1024 pixels and was cooled to –20°C by using Peltier cooling to reduce noise. The ICCD camera was electrically triggered by the Nd:YAG laser pulse after a software-controlled, adjustable time delay. In this way, the intense background radiation initially created by the high-temperature plasma was mostly eliminated, and the atomic/ionic emission lines of the elements were more clearly observed. Usually, spectra from several laser shots (about 40–80) were obtained, and an average was taken to increase the S/N ratio. Samples were manually moved between exposures to prevent crater formation and to avoid other harmful effects of the sample. The spectrum, captured by the ICCD camera, was transferred to the personal computer by a USB cable. WinSpec/32 software, provided by the manufacturer, was used to control all the functions of the gated ICCD camera and the Acton spectrograph [33].

Sample preparation. Aqueous solutions with different known concentrations of Pb (0.5 to 3000 ppm) were prepared in the laboratory by dissolving different Pb salts in de-ionized distilled water. ZnO (UNI-CHEM chemical reagents, China) or zeolite of a fixed amount was chosen as an adsorbent. Then the blend of the adsorbent was dipped into aqueous solutions (of a fixed volume) of different concentrations of Pb salt for 20 h so that a sufficient amount of adsorption could take place. The pH was maintained in the range 2–3 in Pb salt solution to avoid possible precipitation of Pb. Then the solution was filtered to get the adsorbent containing the absorbed Pb salt. After filtering, the adsorbent was dried at 80°C for 2 h. Finally, the sample pellet was prepared using a hand press and a pressure of 80 bars to make the sample reasonably strong. The spectral emission lines of Pb I at the wavelengths of 357.211, 363.958, and 368.319 nm were used for drawing the calibration curves. The three emission lines of Pb I and one emission line of Zn (at 334.448 nm) were brought together in one window using 600 rulings per mm grating. Similar procedures were followed using zeolite as an adsorbent except that the three emission lines of Pb I were normalized with the emission line of Si (390.558 nm) from zeolite.

Results and discussion. In this paper, an attempt has been made to detect and estimate the deleterious Pb dissolved in water in the sub-ppm level using the LIBS technique upon exploiting the unique features of adsorption. A critical task for enabling the sub-ppm detection of heavy metals is to optimize the delay. As far as only the *S/N* ratio is concerned, a delay time of 1700 ns for the gated ICCD detector was found to be optimum for the Pb I line (at 368.319 nm) used for the calibration curve (Fig. 2a). However, our earlier work [8] on arsenic and the current LIBS investigation suggest that the strength of the signal for the atomic lines of Pb is not constant but decreases with increasing delay time of the gated ICCD detector. At a 1700 ns delay, corresponding to the highest *S/N*, the intensity of the Pb I 368.319 nm atomic emission line becomes too low to

be detected at the ppm level of the Pb concentration. Therefore, in the sub-ppm detection of trace elements, both the *S/N* ratio and the signal strength should be given equal weight to optimize the delay time. Therefore, Signal×(*S/N)* as a function of the delay time was also plotted in Fig. 2b, and we obtained an optimized delay time of 650 ns by taking into account both the signal strength and the *S/N* ratio. Likewise, the optimum delay time was found to be 700 ns for both Pb I atomic emission lines at 357.269 and 363.958 nm.

ZnO was primarily used for LIBS investigations because of its superior adsorption capacity, as was found in the case of adsorbing arsenic compounds dissolved in water [8] or quantitative determination of Cr in ink [34]. Different Pb salts such as $PbSO_4$, $Pb(NO_3)_2$, $Pb(CH_3COO)_2 \cdot Pb(OH)_2$, and $PbCl_2$ were used to compare their effectiveness in obtaining the calibration curve with a minimum detectable Pb concentration using the ZnO adsorbent. The selected Pb compounds were directly dissolved in water or titrated with HNO_3 acid to produce Pb complexes easily soluble in water. The pH of all the solutions was maintained around 2 to 2.5.

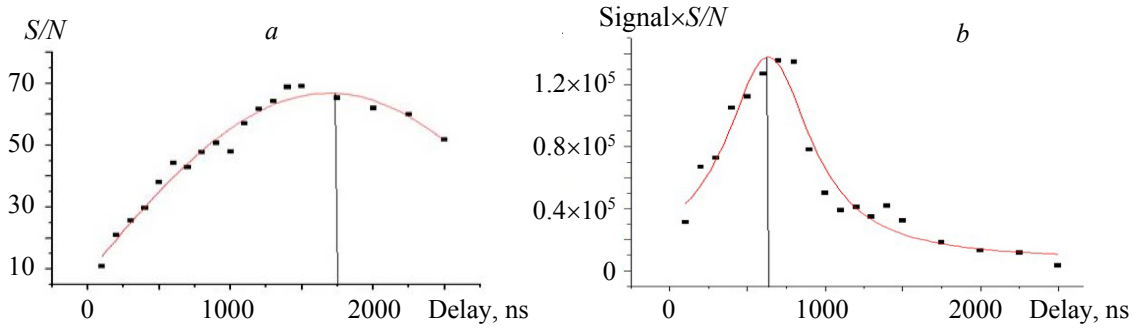

Fig. 2. Optimization of the signal as a function of the delay time. Plots of (a) S/N vs. delay time and (b) Signal×S/N vs. delay time. The gate width was kept fixed at 50 μs.

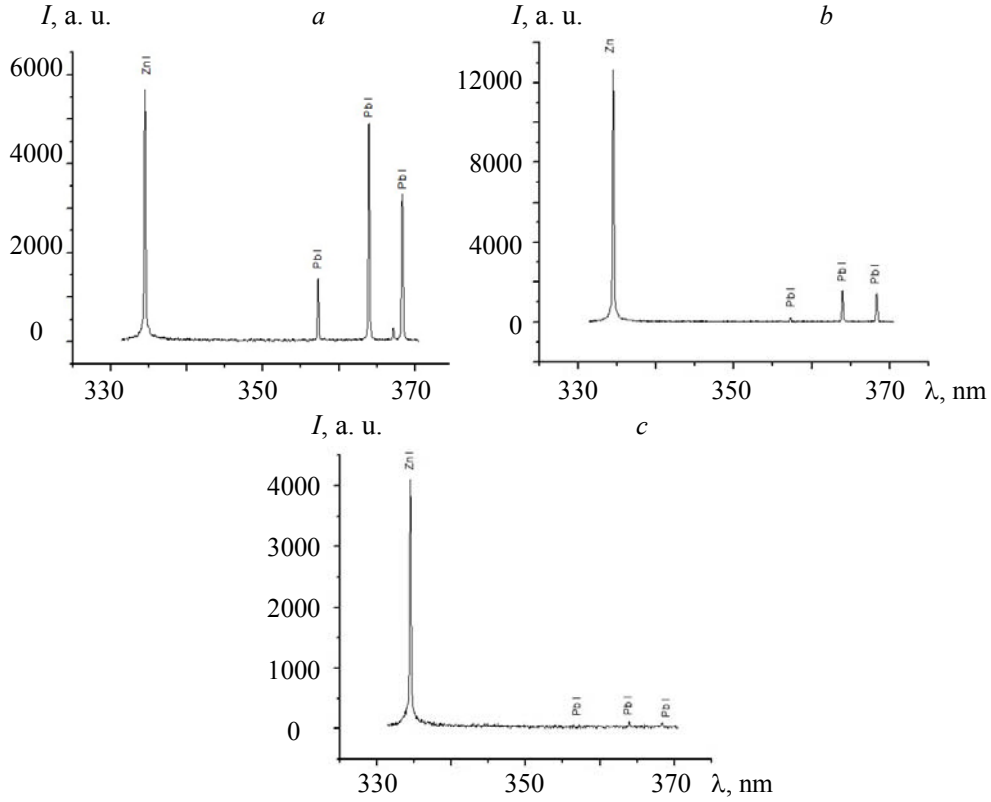

Fig. 3. The LIBS spectra of the added Pb in water at concentrations of (a) 1000, (b) 20, and (c) 0.5 ppm using zinc oxide as an adsorbent in H_2O+$Pb(NO_3)_2$ solution.

The LIBS spectra of the added Pb (using $Pb(NO_3)_2$ salt) in the water at different concentrations using ZnO as the adsorbent are shown in Figs. 3a–c. For obtaining the calibration curves, the line intensities of Pb I at 357.269, 363.269, and 368.319 nm were normalized with one of the simultaneously recorded Zn emission lines at 334.448 nm from the ZnO adsorbent (always at a fixed amount) in the same spectral window (331.5–370.5 nm). The intensity ratio of the Pb I line to that of the Zn line (334.448 nm) versus the concentrations of Pb in water was used for obtaining the calibration curve (Fig. 4). This curve will serve as a future reference curve for the quantitative determination of the unknown concentration of Pb in a liquid matrix such as polluted water bodies in Bangladesh.

The calibration curve exhibited an onset of saturation at 50 ppm when the ZnO adsorbent was used in $Pb(NO_3)_2$ salt solution (Fig. 4a). For concentrations lower than 50 ppm, the adsorption was almost linear, with a 0.99 coefficient of correlation of the straight line. The saturation effect (nonlinear part of the graph) in the adsorption of $Pb(NO_3)_2$ on the surface of the ZnO adsorbent indicates the unavailability of vacancies on the surface of the adsorbent. Therefore, after the saturation, a further increase in the concentration does not cause any significant difference in the adsorption process. This characteristic saturation, also reported by Haider et al. [8], limits the highest concentration detected by this adsorbent-coupled LIBS measurement of trace elements in a liquid for a particular adsorption time. The saturation concentration can be extended by lowering the adsorption time. However, a lower adsorption time increases the LoD. The initial linear part and the subsequent saturation of the calibration curve suggest that these are Langmuir type isotherms.

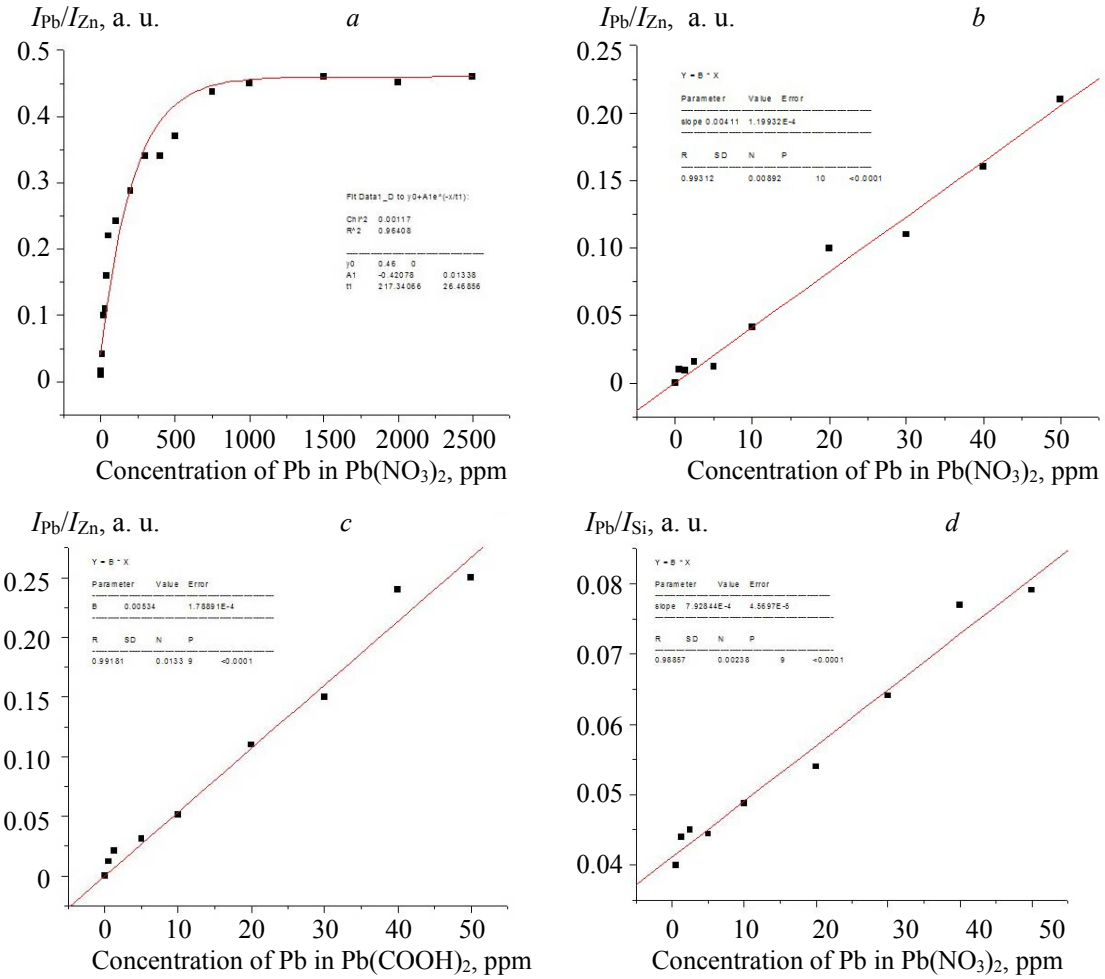

Fig. 4. (a) Saturation effect in the ZnO adsorbent, (b) calibration curve for the determination of the unknown concentration of Pb in the ZnO adsorbent obtained from $Pb(NO_3)_2$ solution using the 368.319 nm Pb I emission line, (c) calibration curve for the Pb adsorbed in ZnO obtained from H_2O+$Pb(CH_3COO)_2{\cdot}Pb(OH)_2$ solution using the 368.319 nm Pb I emission line, and (d) calibration curve for the Pb adsorbed in zeolite obtained from H_2O+$Pb(NO_3)_2$ solution using the 368.319 nm Pb I emission line.

Table 1 summarizes the LoDs and the detection sensitivities in terms of the slopes of the linear parts of the Langmuir isotherm for different absorbents using different Pb salt solutions. In the case of Pb adsorption by ZnO from the $Pb(NO_3)_2$ and $Pb(CH_3COO)_2 \cdot Pb(OH)_2$ solution, the detection limits associated with the 357.211 nm Pb I line were 20 ppm, whereas the detection limits associated with both the 363.958 nm and 368.319 nm Pb I lines were 0.5 ppm. The higher detection limit of 357.211 nm Pb I line can be explained by noting that the relative intensity for the 357.211 nm emission line (35,000) is lower compared to that of the 363.958 and 368.319 nm emission lines (the relative intensities are 50,000 and 70,000 respectively, according to the NIST database [35]).

TABLE 1. Limit of Detection and Slope of the Linear Part of the Calibration Curve for Various Pb Emission Lines Obtained for Different Adsorbents in Solutions of Different Pb Salts

Pb Salt	Pb I emission line, nm	Lowest Detection Limit, ppm	Highest Detection Limit, ppm	The slope of the linear part of the calibration curve, ppm^{-1}
Adsorbent ZnO				
$Pb(NO_3)_2$	357.211	20	50	51.66×10^{-5}
	363.958	0.5		472×10^{-5}
	368.319			411×10^{-5}
$Pb(CH_3COO)_2$ $Pb(OH)_2$	357.211	20	50	77.1×10^{-5}
	363.958	0.5		702×10^{-5}
	368.319			534×10^{-5}
$PbSO_4$	357.211	100	500	2.79×10^{-5}
	363.958	50		10.76×10^{-5}
	368.319			10.35×10^{-5}
$PbCl_2$	357.269	Cannot be detected	500	No graph obtained
	363.958	200		3.569×10^{-5}
	368.319			2.859×10^{-5}
Adsorbent zeolite				
$Pb(NO_3)_2$	357.269	Cannot be detected	50	No graph obtained
	363.958	100		18.4×10^{-5}
	368.319	0.5		79.2×10^{-5}

The LoD was found to vary for various adsorbates. We used four adsorbates such as $PbCl_2$, $PbSO_4$, $Pb(NO_3)_2$, and $Pb(COOH)_2 \cdot Pb(OH)_2$ with the ZnO adsorbent for probing a trace amount of Pb dissolved in water. Table 1 shows that for the same emission line and the same adsorbent, the LoDs for $PbCl_2$ and $PbSO_4$ are 200 and 50 ppm, respectively, whereas for $Pb(NO_3)_2$ and $Pb(COOH)_2 \cdot Pb(OH)_2$, it is 0.5 ppm. The observed higher LoDs for $PbSO_4$ and $PbCl_2$ indicate that these Pb compounds are less suited for adsorption by ZnO. However, Pb $(NO_3)_2$ and $Pb(COOH)_2 \cdot Pb(OH)_2$ show excellent adsorption in ZnO in terms of LoDs, indicating the better suitability of the two salts for constructing the calibration curves upon adsorption. Finally, as the slope of the $Pb(COOH)_2 \cdot Pb(OH)_2$ based calibration curve is higher than that of $Pb(NO_3)_2$, we conclude that the $Pb(COOH)_2 \cdot Pb(OH)_2$ based calibration curve has a better sensitivity than that of $Pb(NO_3)_2$ (Table 1).

An alternative adsorbent, zeolite, was also used for drawing similar calibration curves. For better solubility, $Pb(NO_3)_2$ was chosen to test the adsorption ability of zeolite. In this case, intensities of the same Pb I atomic emission lines (357.211, 363.958, and 368.319 nm) were normalized with that of the Si emission line at 390.558 nm. The spectral window was now set between 355 and 394 nm. For the Pb adsorbed in zeolite, the calibration curve using the Pb I 368.369 nm line yielded an LoD of 0.5 ppm with no visible sign of any saturation of adsorption up to a Pb concentration of 50 ppm, which was almost the same for the Pb adsorbed in the ZnO adsorbent. However, the slopes of the $Pb(NO_3)_2$ calibration curves with the ZnO adsorbent have values greater than the slopes of the $Pb(NO_3)_2$ calibration curves with the zeolite adsorbent (Table 1 and Fig. 4), indicating that ZnO is a better adsorbent than zeolite in terms of the slope of the linear part of the

isotherm and hence the sensitivity of detection. For zeolite, the LoD for the Pb I line at 363.958 nm is much higher (100 ppm) than the corresponding LoD for the 368.319 nm line (0.5 ppm). The LoDs for these two lines with the ZnO adsorbent were identical for all the Pb salt complexes investigated. This measured difference in the case of zeolite may be due to the quenching of the 363.958 nm emission line intensity by some constituents of zeolite. However, further studies of zeolite as an adsorbent are needed to explain the underlying reason for this difference in LoDs for the two lines, which can be done in a separate investigation.

For both the adsorbents and for all the four adsorbates used, the adsorption curves as a function of the adsorbate concentration in water followed the Langmuir type isotherms. The lowest detection limit and the slope of the linear part of the adsorption isotherm varied for various adsorbents, adsorbates, and the different Pb I emission lines used.

The LoD for Pb in an aqueous solution in the current study using LIBS coupled with adsorption technique was found to be 0.5 ppm. It should be noted that the detection of Pb in an aqueous solution is more challenging than arsenic [8] because the atomic mass of Pb is 2.77 times larger than that of arsenic (207.2 vs.74.9216). Therefore, the aqueous solution of Pb has a smaller number of atoms compared to the aqueous solution of arsenic for the identical ppm by weight, rendering the detection of Pb in an aqueous solution more challenging.

Because these results were achieved without sample pretreatment, the LIBS technique coupled with adsorption has a great potential for practical application in the elemental analysis of sub-ppm Pb detection in a liquid matrix [17]. Therefore, the LIBS technique coupled with adsorption shows its greatest advantages compared to other complex analytical methods for sub-ppm level Pb detection in a liquid, such as LIBS coupled with LIF [20]. The improvement of the trace amount detection limit of a toxic element like Pb in aqueous solutions using LIBS coupled with adsorption will be extremely useful for monitoring the Pb contamination in polluted water bodies adjacent to industries. It should be noted that the Pb detection limit could also be increased by increasing the concentration of Pb in the water sample by pre-boiling [20, 31].

Conclusions. We obtained herein calibration curves for two types of adsorbents such as ZnO and zeolite using four adsorbates such as $PbSO_4$, $Pb(NO_3)_2$, $Pb(CH_3COO)_2 \cdot Pb(OH)_2$, and $PbCl_2$. The adsorption curves as a function of the adsorbate concentration in water followed the Langmuir type isotherms. The calibration curves can, in turn, be employed to estimate the unknown concentration of Pb in natural water samples. The accurate trace element concentration can only be found below the saturation limit. The slope of the linear part of the adsorption isotherm (calibration curve) varied for different adsorbents, adsorbates, and Pb I emission lines. ZnO was found to be a better adsorbent than zeolite in terms of the slope of the linear part of the isotherm and hence the sensitivity of detection. The ZnO adsorbent also showed better results in terms of LoDs for Pb in water (0.5 ppm) for both lines of Pb I 363.958 and 368.319 nm. In the adsorption method, the concentration of trace elements on the surface of the adsorbent is many times higher than that of the liquid, which enhances the S/N ratio of the LIBS signal, enabling the trace element detection in water. This novel application of LIBS can be universally applied for the detection of any trace element in aqueous solutions.

The LoD was pushed down further to 4 ppb and 3.5 ppb by Ma et al. [29] and Lie et al. [27] using surface-enhanced LIBS and metal-chelate induced nanoparticle aggregation enhanced LIBS, respectively. However, the present study used a straightforward adsorption technique to enhance the detection efficiency of trace elements in an aqueous solution by LIBS and push it down to the sub-ppm-level. The LoD for the Pb in an aqueous solution in the present LIBS experiment coupled with the adsorption technique was 0.5 ppm, which is an order of magnitude lower than the standard permissible limit of 5 ppm or less for industrial waste as suggested by the Environmental Protection Agency (EPA) [20, 31]. Therefore, the present simple LIBS technique coupled with adsorption is good enough for most practical purposes.

Acknowledgements. The experimental work was performed in the Nonlinear Optics and Laser Spectroscopy Laboratory of the Center for Advanced Research in Sciences (CARS) of Dhaka University.

REFERENCES

1. L. J. Radziemski, D. A. Cremers, *Laser-Induced Plasmas and Applications*, Marcel Dekker, New York (1989).
2. D. A. Cremers, F. Y. Yueh, J. P. Singh, H. Zhang, *Encyclopedia of Analytical Chemistry: Applications, Theory and Instrumentation,* John Wiley & Sons, Ltd. (2006).
3. A. W. Miziolek, V. Palleschi, I. Schechter, *Laser Induced Breakdown Spectroscopy*, Cambridge University Press (2006).
4. A. Haider, Z. Khan, *Opt. Laser Technol.*, **44**, No. 6, 1654–1659 (2012).

5. K. Abedin, A. Haider, M. Rony, Z. Khan, *Opt. Laser Technol.*, **43**, No. 1, 45–49 (2011).
6. R. S. Harmon, J. Remus, N. J. McMillan, C. McManus, L. Collins, J. L. Gottfried Jr., F. C. DeLucia, A. W. Miziolek, *Appl. Geochem*., **24**, No. 6, 1125–1141 (2009).
7. S. Morel, N. Leone, P. Adam, J. Amouroux, *Appl. Opt.*, **42**, No. 30, 6184–6191 (2003).
8. A. F. M. Y. Haider, M. H. Ullah, Z. H. Khan, F. Kabir, K. M. Abedin, *Opt. Laser Technol.*, **56**, 299–303 (2014).
9. A. C. Samuels, F. C. DeLucia, K. L. McNesby, A. W. Miziolek, *Appl. Opt.*, **42**, No. 30, 6205–6209 (2003).
10. A. R. Boyain-Goitia, D. C. Beddows, B. C. Griffiths, H. H. Telle, *Appl. Opt*., **42**, No. 30, 6119–6132 (2003).
11. X. Fang, S. R. Ahmad, M. Mayo, S. Iqbal, *Laser Med. Sci*., **20**, No. 3-4, 132–137 (2005).
12. Z. A. Arp, D. A. Cremers, R. C. Wiens, D. M. Wayne, B. Sallé, S. Maurice, *Appl. Spectrosc*., **58**, No. 8, 897–909 (2004).
13. A. K. Rai, F.-Y. Yueh, J. P. Singh, *Appl. Opt*., **42**, No. 12, 2078–2084 (2003).
14. D. A. Cremers, L. J. Radziemski, T. R. Loree, *Appl. Spectrosc*., **38**, No. 5, 721–729 (1984).
15. R. L. Vander Wal, T. M. Ticich, J. R. West, P. A. Householder, *Appl. Spectrosc*., **53**, No. 10, 1226–1236 (1999).
16. G. Arca, A. Ciucci, V. Palleschi, S. Rastelli, E. Tognoni, *Appl. Spectrosc*., **51**, No. 8, 1102–1105 (1997).
17. C. Chen, G. Niu, Q. Shi, Q. Lin, Y. Duan, *Appl. Opt*., **54**, No. 28, 8318–8325 (2015).
18. J.-S. Huang, H.-T. Liu, K.-C. Lin, *Anal. Chim. Acta*, **581**, No. 2, 303–308 (2007).
19. C. Janzen, R. Fleige, R. Noll, H. Schwenke, W. Lahmann, J. Knoth, P. Beaven, E. Jantzen, A. Oest, P. Koke, *Spectrochim. Acta B, Atom. Spectrosc*., **60**, No. 7-8, 993–1001 (2005).
20. S. L. Lui, Y. Godwal, M. T. Taschuk, Y. Y. Tsui, R. Fedosejevs, *Anal. Chem*., **80**, No. 6, 1995–2000 (2008).
21. D. Zhu, J. Chen, J. Lu, X. Ni, *Anal. Methods*, **4**, No. 3, 819–823 (2012).
22. R. Knopp, F. Scherbaum, J. Kim, *Fresenius' J. Anal. Chem.*, **355**, No. 1, 16–20 (1996).
23. Z. Chen, H. Li, M. Liu, R. Li, *Spectrochim. Acta B, Atom. Spectrosc*., **63**, No. 1, 64–68 (2008).
24. Q. Lin, Z. Wei, M. Xu, S. Wang, G. Niu, K. Liu, Y. Duan, J. Yang, *RSC Adv.*, **4**, No. 28, 14392–14399 (2014).
25. Z. Chen, H. Li, F. Zhao, R. Li, *J. Anal. Atom. Spectrom*., **23**, No. 6, 871–875 (2008).
26. D. D. Pace, C. D'Angelo, D. Bertuccelli, G. Bertuccelli, *Spectrochim. Acta B, Atom. Spectrosc.*, **61**, No. 8, 929–933 (2006).
27. X. Liu, Q. Lin, Y. Tian, W. Liao, T. Yang, C. Qian, T. Zhang, Y. Duan, *J. Anal. Atom. Spectrom*., **35**, No. 1, 188–197 (2020).
28. H. Loudyi, K. Rifai, S. Laville, F. Vidal, M. Chaker, M. Sabsabi, *J. Anal. Atom. Spectrom*., **24**, No. 10, 1421–1428 (2009).
29. S. Ma, Y. Tang, Y. Ma, Y. Chu, F. Chen, Z. Hu, Z. Zhu, L. Guo, X. Zeng, Y. Lu, *Opt. Express*, **27**, No. 10, 15091–15099 (2019).
30. https://www.who.int/news-room/fact-sheets/detail/lead-poisoning-and-health.
31. http://www.epa.gov/OGWDW/standard.
32. A. F. M. Y. Haider, M. K. Ira, Z. Khan, K. Abedin, *J. Anal. Atom. Spectrom*., **29**, No. 8, 1385–1392 (2014).
33. A. F. M. Y. Haider, B. Rahman, Z. H. Khan, K. M. Abedin, *Environ. Eng. Sci*., **32**, No. 4, 284–291 (2015).
34. J. Wei, T. Zhang, J. Dong, L. Sheng, H. Tang, X. Yang, H. Li, *Chem. Res. Chin. Univ*., **31**, No. 6, 909–913 (2015).
35. https://www.physics.nist.gov/PhysRefData/ASD/lines_form.html.